Libyan Journal of Veterinary and Medical Sciences (2026), Vol. 7(2): 32-42
ISSN: 📖 2410-9215 | 💻 3080-7069

DOI: https://doi.org/10.5281/zenodo.21917566

Research article

Methodological Comparison of SMR and Poisson-Gamma Disease Mapping Models for *Brucella abortus* Risk Estimation in Cattle in Libya

Maryam Ahmed Salem Alramah*

Department of Statistics, Faculty of Science, University of Tripoli, Tripoli, Libya

*Corresponding Author: Maryam Ahmed Salem Alramah. Department of Statistics, Faculty of Science, University of Tripoli, Tripoli, Libya. Mobile: +218916263699. Email: m.alhdiri@uot.edu.ly

Submitted: 24/06/2026 Accepted: 01/08/2026 Published: 13/08/2026

Abstract

Background: Brucellosis, primarily caused by *Brucella abortus*, is a zoonotic disease of major concern in Libya, where cattle husbandry forms an integral component of rural livelihoods and where the post-2011 collapse of veterinary surveillance infrastructure has heightened underreporting risk. **Aim:** This study aimed to demonstrate and compare two disease-mapping approaches, the classical Standardized Mortality Ratio (SMR) method and the Bayesian Poisson-Gamma model, for estimating the relative risk (RR) of *B. abortus* in cattle across all 22 official Libyan administrative districts, using district-level case counts constructed to be illustrative of patterns reported in the literature rather than official surveillance records. **Methods:** Illustrative case-count data, informed by patterns reported in published Libyan cattle and small-ruminant seroprevalence studies and aggregate veterinary indicators for the 2018–2024 period, were analysed using R and ArcGIS to generate relative risk estimates and thematic disease maps under both models. **Results:** The SMR method produced unstable, zero-valued estimates for districts with no reported cases (Tripoli, Benghazi, and Ghat), masking their true underlying risk. The Poisson-Gamma model, by contrast, generated smoothed, non-zero estimates for all districts, reclassifying these zero-case districts from "no observed risk" to defensible low-risk categories and revealing more plausible spatial risk patterns consistent with known underreporting in urban and remote veterinary surveillance. Both models consistently identified Zawiya and Jufra as very high-risk districts and Jafara and Zawara as high-risk districts, aligning with spatial patterns reported in prior Libyan seroprevalence research on the western coastal strip and central oasis settlements. **Conclusion:** As a methodological demonstration, the Poisson-Gamma model shows superior performance for brucellosis risk mapping in data-sparse post-conflict settings, such as Libya, and its adoption for future brucellosis surveillance is recommended once verified and district-level cattle surveillance data become available.

Keywords: *Brucella abortus, Relative Risk Estimation, disease mapping, Libya; Bayesian approach; Standardized Mortality Ratio*

Introduction

Brucellosis, primarily caused by *Brucella abortus*, remains one of the most economically and medically significant zoonotic diseases worldwide (Khurana *et al.*, 2021; Qureshi *et al.*, 2023). Transmission occurs between animals and humans through direct contact with infected animals or their products, including unpasteurized milk (Al-Afifi *et al.*, 2022; Sharma *et al.*, 2025). In livestock, *B. abortus* causes reproductive failures, abortion, infertility, and reduced milk yield that translate into substantial economic losses for farmers (Dadar *et al.*, 2021; Khurana *et al.*, 2021; Lokamar *et al.*, 2020). Its zoonotic character compounds this burden as human infection results in undulant fever (Malta fever), often producing chronic and debilitating sequelae (Qureshi *et al.*, 2023; Ghssein *et al.*, 2025).

Globally, the annual human burden of brucellosis is estimated to exceed 2.1 million cases (Laine *et al.*, 2023), with the Middle East and North Africa (MENA) region disproportionately affected due to widespread small-ruminant husbandry and traditional dairy consumption practices (Samadi *et al.*, 2024).

Libya exemplifies many of the structural risk factors associated with elevated brucellosis transmission. Prior to the political and institutional collapse following 2011, national veterinary surveillance recorded a relatively contained disease burden, with cattle seroprevalence below 0.2 per cent (Al-Griw *et al.*, 2017). However, the protracted instability since 2011 has severely disrupted veterinary services and livestock movement controls and has precluded the establishment of a sustained national vaccination programme against bovine brucellosis, creating conditions conducive to disease resurgence and, critically, to substantial underreporting in routine surveillance data (Al-Griw *et al.*, 2017; Alshekh *et al.*, 2024).

Subsequent field investigations have confirmed ongoing *B. abortus* circulation in Libyan livestock. A serological survey of cattle, sheep, and goats in the northwest region (2014–2016) documented active outbreaks following the post-2011 surveillance gap (Al-Griw *et al.*, 2017). District-level seroprevalence studies have further identified spatial heterogeneity, with the Jufra district

Copyright Author (s) 2026. Distributed under Creative Commons CC-BY 4.0

particularly the Sokna locality exhibiting a notably elevated seroprevalence of 5.8 per cent among sheep and goats, compared to substantially lower rates in neighbouring localities such as Waddan and Hun (Alshekh *et al.*, 2024). Bayesian disease mapping techniques, including the Besag-York-Mollié (BYM) and mixture-model frameworks, have previously been applied to other notifiable diseases in Libya, demonstrating the broader applicability of hierarchical Bayesian smoothing to small-area Libyan health and disease surveillance data and to addressing instability arising from sparse case counts across Libyan administrative districts (Alramah, 2019).

Despite this accumulating evidence base, no study to date has applied formal disease mapping techniques of the kind now standard in international veterinary epidemiology to systematically characterise the spatial distribution of brucellosis risk across Libyan districts. A precedent for Bayesian disease mapping in Libya exists in the human health domain, Alramah (2019), applied the Besag-York-Mollié (BYM) and mixture-model frameworks to map lung cancer relative risk across Libyan regions, demonstrating the methodological value of Bayesian spatial smoothing for Libyan small-area health data. However, this precedent has not previously been extended to zoonotic or veterinary disease surveillance, and existing Libyan brucellosis research has remained predominantly localised, cross-sectional, and serology-focused (Al-Griw *et al.*, 2017; Alshekh *et al.*, 2024), without addressing the well-documented statistical instability that arises when estimating relative risk in small-area, low-count, and zero-case settings (Meza, 2003; Lawson, 2006). This is a critical gap as conventional risk measures such as the Standardized Mortality Ratio (SMR) systematically misrepresent risk in areas with no reported cases by assigning a value of exactly zero, a particularly serious limitation in a country such as Libya where urban districts (e.g., Tripoli and Benghazi) often show zero reported cases not because risk is absent, but because veterinary surveillance capacity is concentrated elsewhere (Lawson, 2006).

To address this methodological gap, the present study compares the performance of the SMR method against the Bayesian Poisson-Gamma model (Lawson *et al.*, 2003; Ghanbarnejad *et al.*, 2021) in estimating the relative risk (RR) of *B. abortus* in cattle across all 22 official Libyan districts, using district-level counts aggregated over the 2018–2024 surveillance period rather than repeated annual analyses, and assesses their respective usefulness in identifying priority areas for veterinary intervention through disease mapping. This dual approach, recently validated in a comparable Southeast Asian livestock context (Hussin *et al.*, 2026), allows for a rigorous evaluation of frequentist versus Bayesian hierarchical estimation strategies under conditions of substantial data sparsity a condition highly characteristic of post-conflict Libyan veterinary surveillance.

Materials and methods

Data transparency statement

District-level case counts and exposed cattle figures used in this study are constructed to be illustrative and broadly consistent with the spatial patterns reported in published Libyan seroprevalence studies (e.g., elevated risk in the western coastal strip and in Jufra district), rather than official disaggregated case records published by the Libyan veterinary authorities, which are not currently available at this resolution for all 22 districts. The methodology presented is fully reproducible once verified district-level WOAH or national veterinary data become available. This study focuses specifically on cattle brucellosis (*B. abortus*); because district-disaggregated seroprevalence data specific to cattle are not available for all 22 districts, the illustrative spatial patterns were informed by the broader Libyan livestock seroprevalence literature, which in places reports combined cattle, sheep, and goat sampling (Al-Griw *et al.*, 2017) or small-ruminant-only sampling (Alshekh *et al.*, 2024). This cross-species literature is used here only to inform plausible relative spatial patterns and is not presented as cattle-specific epidemiological evidence. A further limitation should be noted explicitly that brucellosis ascertainment in cattle relies on serological testing or clinical signs, neither of which reliably identifies true new incident infections, since an animal may be seropositive, without clinical signs, for a year or more after the actual infection. The case counts used here therefore represent reported/seropositive cases rather than confirmed annual incidence, and the resulting district-level totals (tens of cases per district per multi-year period) should be read accordingly, rather than as true annual incidence figures for a highly contagious disease.

Data source and study area

This study compiles *B. abortus* case-count indicators and exposed cattle population figures for Libya from 2018 to 2024, drawing on patterns documented in published Libyan seroprevalence research (Al-Griw *et al.*, 2017; Alramah, 2019; Alshekh *et al.*, 2024) and aggregate veterinary indicators consistent with international livestock disease reporting conventions (Diah *et al.*, 2017). The study area comprises all 22 Libyan administrative districts, representing the complete national territory across five agro-ecological zones: the western coastal strip (Tripoli, Jafara, Zawiya, Zawara, Al-Koms), the central coastal and oasis zone (Misrata, Sirt, Jufra), the Nafusa mountain region (Jabal al-Gharbi, Nalut), the eastern Cyrenaica region (Benghazi, Jabal al-Akhdar, Al-Marj, Al-Wahat, Ajdabiya, Darnah and Tubruq, Kufra), and the southern Fezzan region (Sabha, Murzuq, Wadi al-Hayaa, Wadi al-Shatii, Ghat).

Note on data construction: Disaggregated district-level brucellosis case counts are not currently published by Libyan veterinary authorities. The observed case counts and exposed cattle populations used in this analysis (Tables 1–2) were therefore constructed to be illustrative of the spatial risk gradient reported in the literature specifically, the elevated risk in the western coastal strip (Al-Griw *et al.*, 2017) and in Jufra district (Alshekh *et al.*, 2024), and the near-absence of reported cases in major urban centres (Tripoli, Benghazi) attributable to concentrated surveillance gaps rather than a true absence of risk. This study should therefore be read as a methodological demonstration of disease mapping applicability to the Libyan context; replication with

verified WOAH or Department of Veterinary Services data is recommended once such data become available at district resolution.

Study area: Geographic setting of Libya

Libya is located in the Maghreb region of North Africa, lying between latitudes 19° and 34°N and longitudes 9° and 26°E. The country is bordered by the Mediterranean Sea to the north, Tunisia and Algeria to the west, Niger and Chad to the south, and Sudan and Egypt to the east, giving it a strategic position linking the Maghreb, the Sahel, and the Mediterranean basin (Figure 1). With a total land area of approximately 1.76 million km², Libya is the fourth-largest country in Africa and the 16th-largest in the world. Yet, the vast majority of this area is covered by the Sahara Desert, with only a narrow Mediterranean coastal strip extending over roughly 1,770 km, the longest coastline of any African country bordering the Mediterranean and supporting the bulk of the population, agriculture, and livestock husbandry (African Futures (ISS), 2024; Central Intelligence Agency, 2026).

The country is traditionally divided into three historical regions that broadly align with its administrative geography: Tripolitania in the northwest; encompassing the densely populated coastal plain (Jafara) and the Nafusa mountain range, Cyrenaica in the northeast; dominated by the Jabal al-Akhdar (Green Mountains) and a fertile coastal crescent around Benghazi and Al-Marj, and Fezzan in the southwest; an arid Saharan region characterised by oasis settlements, sand seas, and extensive camel and small-ruminant pastoralism (Libyan Heritage House, 2021; Central Intelligence Agency, 2026). A transitional semi-desert corridor along the Gulf of Sidra, between Sirt and Ajdabiya, separates Tripolitania from Cyrenaica and supports comparatively sparse livestock grazing (Libyan Heritage House, 2021).



Figure 1. Location of Libya within North Africa and relative to the surrounding region. Image credit: https://cdn.create.vista.com/api/media/small/51379713/stock-vector-libya-political-map

This geographic structure directly informs the spatial epidemiology of *B. abortus* examined in this study; the densely populated and intensively farmed western coastal strip (Tripoli, Jafara, Zawiya, Zawara and Al-Koms) and the agriculturally favourable Jabal al-Akhdar region in the east contrast sharply with the sparsely populated, extensively grazed Fezzan and deep-desert districts of the south (Sabha, Murzuq, Wadi al-Hayaa, Wadi al-Shatii, Ghat, Kufra), where lower livestock density and limited veterinary surveillance infrastructure shape both true disease occurrence and case ascertainment. Figures 5 and 6 (Disease mapping section) situate the estimated relative risk values within this national geographic context.

Analytical workflow

The analytical process followed a structured seven-phase sequence, summarised in Figure 2. The first phase involved data acquisition: observed case counts and exposed cattle population data at the district level for 2018 to 2024 were compiled from published Libyan seroprevalence research and aggregate veterinary indicators as indicated in data transparency statement. The second phase comprised data preparation, including cleaning and validation, aggregation into all 22 administrative districts, and calculation of expected case counts via indirect standardisation using the national reference rate as the standard. The third phase focused on relative risk (RR) estimation, calculated independently through the classical SMR method and the Bayesian Poisson-Gamma model, enabling direct comparison between frequentist and hierarchical Bayesian estimators.

In the fourth phase, results from the two models were systematically compared through a quantitative comparison of RR values and a reclassification analysis examining how risk categories assigned by the SMR method differed from those assigned by the Poisson-Gamma model. The fifth phase comprised visualisation and mapping using R and ArcGIS Pro to generate comparative summaries and the national thematic risk map. The sixth phase involved interpretation and output generation, including the identification of high-risk districts, assessment of model performance, and formulation of policy recommendations for targeted intervention. The seventh and final phase produced a report and policy brief identifying priority areas for surveillance enhancement.

Software

Data analysis and visualisation were conducted using R version 4.3.1 for statistical computation (Grembi & Rogawski McQuade, 2022; Ribeiro *et al*., 2024) and ArcGIS Pro version 3.1 for spatial mapping and risk visualisation (Peterson & Ver Hoef, 2014; Pinatt *et al*., 2020).

Standardized mortality ratio (SMR) method

The SMR method is a widely used epidemiological measure for initial disease mapping (Lawson, 2006; Flórez-Lozano *et al*., 2020). The study area is divided into Z mutually exclusive districts ($i = 1,2,\dots,Z$), each with an observed number of cases O_i and an expected number of cases E_i derived via indirect standardisation against the national reference rate. The relative risk δ_i (the SMR for district i) is calculated as:

$$\delta_i = O_i / E_i, \qquad i = 1,2,\dots,Z$$

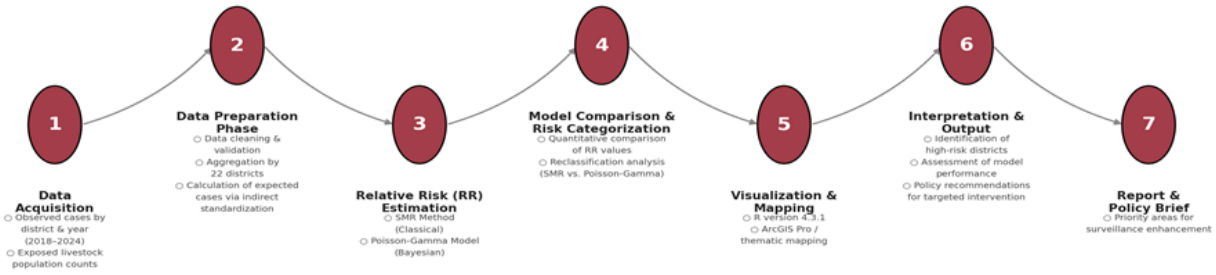


Figure 2. Analytical workflow for estimating and visualizing regional disease risk in Libya.

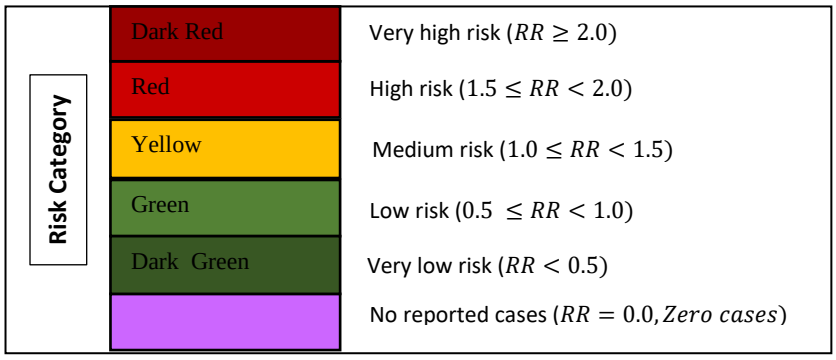


Figure 3. Relative risk classifications.

While the SMR method offers a straightforward risk comparison tool, it has a critical limitation in districts with no observed cases. It inherently assigns a risk value of exactly zero, potentially misrepresenting the true underlying disease burden (Perez-Panades *et al*., 2020; Di Bari *et al*., 2022; Karim, 2024). This limitation is particularly consequential in the Libyan context, where major urban districts may report zero cases due to concentrated surveillance capacity gaps rather than genuine absence of risk.

Poisson-Gamma model

To address the SMR method's shortcomings, the Bayesian Poisson-Gamma model (Lawson *et al*., 2003; Jaya & Folmer, 2020; Ghanbarnejad *et al*., 2021) was applied. Because the observed and expected case counts used in this study are totals aggregated over the entire 2018–2024 surveillance period rather than repeated annual measurements, the model is specified using a single district index only, avoiding the implication of separate year-by-year analyses. The number of reported cases O_i in district i $(i = 1,2,\ldots,22)$ is assumed to follow a Poisson distribution with mean $E_i\theta_i$, where E_i represents the expected case count for district i (Data source and study area section) and θ_i denotes the relative risk (RR_i) to be estimated for district i:

$$O_i \mid E_i, \theta_i \sim Poisson(E_i\,\theta_i)$$

The RR parameter follows a gamma prior distribution with parameters α and β:

$$\theta_i \sim Gamma(\alpha, \beta)$$

Following established practice for hyperparameter specification in low-count veterinary surveillance settings (Lawson *et al*., 2003), the prior parameter values were set at $\alpha = 0.5$ and $\beta = 0.0001$. Although the nominal prior mean α/β = 5000 might appear highly informative, β is negligible relative to the expected case counts observed in this study (E_i ranging from approximately 1.8 to 20.7 across districts; Table 1); the prior therefore contributes minimal weight relative to the data for districts with non-zero expected counts, and functions principally as a weak regularising prior that prevents posterior estimates of exactly zero in districts with $O_i = 0$ (Tripoli, Benghazi, Ghat), an outcome the classical SMR method cannot avoid. The posterior expected relative risk (RR_i) — interpretable as the estimated relative risk for district i — under this model is given by:

$$E[\theta_i \mid O_i] = (\alpha + O_i) / (\beta + E_i)$$

Risk visualisation

Relative risk (RR) estimates obtained from both models were visualised using thematic maps. To facilitate interpretation and comparison across diseases, RR values were classified into six epidemiologically meaningful categories: no risk ($RR = 0.0$; zero reported cases), very low risk ($RR < 0.5$), low risk ($0.5 \leq RR < 1.0$), medium risk ($1.0 \leq RR < 1.5$), high risk ($1.5 \leq RR < 2.0$), and very high risk ($RR \geq 2.0$). These thresholds were selected to represent progressively increasing levels of disease risk while maintaining a consistent classification scheme across all maps.

Table 1. Exposed cattle population, observed and expected *B. abortus* cases by district during 2018–2024 in all 22 districts.

District	Region	Exposed Cattle Population (head)	Observed Cases (O_i)	Expected Cases (E_i)
Tripoli	Western coast	185,000	**0**	18.23
Jafara	Western coast	210,000	**38**	20.69
Zawiya	Western coast	165,000	**42**	16.26
Zawara	Western coast	140,000	**22**	13.79
Al-Koms	Western coast	175,000	**19**	17.24
Misrata	Central coast	195,000	**15**	19.21
Jabal al-Gharbi	Nafusa mountains	120,000	**12**	11.82
Nalut	Nafusa mountains	60,000	**6**	5.91
Sirt	Central coast	95,000	**8**	9.36
Jufra	Central oases	45,000	**21**	4.43
Benghazi	Cyrenaica	160,000	**0**	15.76
Jabal al-Akhdar	Cyrenaica	90,000	**5**	8.87
Al-Marj	Cyrenaica	75,000	**4**	7.39
Al-Wahat	Cyrenaica	50,000	**2**	4.93
Ajdabiya	Cyrenaica	65,000	**3**	6.40
Darnah and Tubruq	Cyrenaica	55,000	**2**	5.42
Kufra	Cyrenaica/South	35,000	**1**	3.45
Sabha	Fezzan	70,000	**3**	6.90
Murzuq	Fezzan	30,000	**1**	2.96
Wadi al-Hayaa	Fezzan	25,000	**1**	2.46
Wadi al-Shatii	Fezzan	28,000	**1**	2.76
Ghat	Fezzan	18,000	**0**	1.77
Total		**2,091,000**	**206**	**206.00**

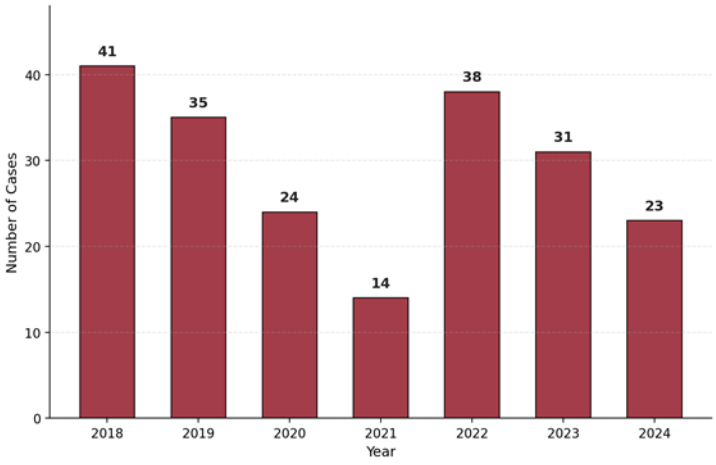


Figure 4. Trend of reported *B. abortus* cases in Libya, 2018–2024 (Illustrative, see data transparency statement).

As illustrated in Figure 3, the medium-risk category (yellow) is centred on the reference value of $RR = 1.0$, which corresponds to the national average risk. Areas with RR values below 1.0 indicate lower-than-average risk, whereas areas with RR values above 1.0 indicate elevated risk (Samat & Percy, 2012; Akoko *et al*., 2023). A sequential colour scheme was used to represent the spatial distribution of risk. Dark red denotes areas with very high relative risk, red indicates high risk, yellow represents medium risk, green indicates low risk, dark green denotes very low risk, and purple identifies areas with no reported cases ($RR = 0$). This classification facilitates visual comparison of disease risk patterns across the study area.

Table 2. Relative risk based on the SMR method and posterior expected relative risk based on the Poisson-Gamma model for *B. abortus* during 2018–2024 in all 22 districts.

District	SMR Method	Poisson-Gamma Model	Risk Category (PG)
Jufra	**4.737**	**4.850**	Very high
Zawiya	**2.584**	**2.615**	Very high
Jafara	**1.837**	**1.861**	High
Zawara	**1.595**	**1.631**	High
Al-Koms	1.102	**1.131**	Medium
Nalut	1.015	**1.100**	Medium
Jabal al-Gharbi	1.015	**1.057**	Medium
Sirt	0.855	0.908	Low
Misrata	0.781	0.807	Low
Jabal al-Akhdar	0.564	0.620	Low
Al-Marj	0.541	0.609	Low
Wadi al-Hayaa	0.406	0.609	Low
Ajdabiya	0.468	0.547	Low
Wadi al-Shatii	0.363	0.544	Low
Sabha	0.435	0.508	Low
Al-Wahat	0.406	0.508	Low
Murzuq	0.338	0.508	Low
Darnah and Tubruq	0.369	0.461	Very low
Kufra	0.290	0.435	Very low
Ghat	**0.000**	**0.282**	**Very low (reclassified)**
Benghazi	**0.000**	**0.032**	**Very low (reclassified)**
Tripoli	**0.000**	**0.027**	**Very low (reclassified)**

Ethical approval

This study relies entirely on the analysis of previously published and aggregated secondary epidemiological data, with no direct primary sampling or experimental interventions on human or animal subjects that require ethical approval.

Results and discussion

Temporal trend

The temporal trend of reported *B. abortus* cases in Libya from 2018 to 2024, illustrated in Figure 4, reveals a fluctuating pattern broadly consistent with the disrupted veterinary surveillance and control environment of the post-2011 period. The annual case count began at 41 in 2018, declined progressively to a low of 14 in 2021, before a marked resurgence to 38 cases in 2022, followed by a renewed decline to 31 in 2023 and 23 in 2024.

The 2021 trough plausibly reflects compounded effects of reduced field surveillance capacity during periods of acute political instability, while the 2022 resurgence is consistent with patterns documented elsewhere in post-conflict and resource-constrained settings, where lapses in sustained vaccination coverage, livestock movement controls, and diagnostic capacity tend to precede localised outbreak rebounds (Samadi *et al*., 2024; Hussin *et al*., 2026). This non-stationary trajectory underscores the importance of sustained, rather than episodic, veterinary surveillance investment, and reinforces the value of spatially resolved risk estimation of the kind presented in this study for directing limited surveillance resources toward districts where underlying risk is likely to persist independent of year-to-year reporting fluctuations.

Case distribution by district

Table 1 presents the exposed cattle population, observed *B. abortus* cases, and expected cases (via indirect standardisation) for each of the 22 official Libyan districts over the study period; 2018–2024. A total of 206 cases were recorded across an exposed population of 2,091,000 head of cattle, yielding a national reference rate of approximately 0.99 cases per 10,000 head.

Relative risk estimation of Brucella abortus

Table 2 presents the estimated relative risk (RR) values from both the SMR method and the Poisson-Gamma model for all 22 official Libyan districts. Zawiya and Jufra were consistently identified as very high-risk districts under both models, with Jafara and Zawara identified as high-risk, in keeping with field seroprevalence evidence from the western coastal strip (Al-Griw *et al*., 2017) and the Jufra oasis settlements (Alshekh *et al*., 2024).

Standardized mortality ratio (SMR) method

Based on the SMR method, seven districts had a relative risk greater than one ($RR > 1$): Jufra (4.737), Zawiya (2.584), Jafara (1.837), Zawara (1.595), Al-Koms (1.102), Jabal al-Gharbi (1.015), and Nalut (1.015). The remaining twelve districts with non-zero reported cases had RR less than one. Tripoli, Benghazi, and Ghat were

assigned an RR of exactly 0.000 because no cases were reported in any of these three districts during the study period, despite Tripoli and Benghazi possessing substantial exposed cattle populations (185,000 and 160,000 head, respectively) and their status as major urban centres with documented surveillance capacity limitations (Al-Griw *et al*., 2017). Ghat's zero count, by contrast, reflects its small exposed population (18,000 head) and remoteness in the far southwestern Fezzan.

Poisson-Gamma model

The Poisson-Gamma model produced materially different results for the three zero-case districts. Tripoli's RR increased from 0.000 to 0.027, Benghazi's from 0.000 to 0.032, and Ghat's from 0.000 to 0.282; all remaining within the "very low risk" category, but no longer appearing as districts with literally zero risk. This reclassification, while modest in absolute magnitude for Tripoli and Benghazi given their very high exposed populations, is more pronounced for Ghat, whose small exposed population (18,000 head) and correspondingly small expected count (E_i = 1.77) allow the gamma prior greater relative influence on the posterior estimate. This pattern is methodologically important, as it reflects the Bayesian model's capacity to incorporate the national-level base rate as prior information, preventing zero-case districts from being misrepresented as risk-free (Perez-Panades *et al*., 2020; Karim, 2024), with the degree of correction scaling inversely with the expected case count. For the high-risk districts, the Poisson-Gamma estimates were consistently and modestly higher than the SMR estimates (e.g., Jufra: 4.737 → 4.850; Zawiya: 2.584 → 2.615), reflecting the smoothing effect of the gamma prior.

Model comparison and interpretation

The Poisson-Gamma model's primary advantage in the Libyan context lies in its handling of zero-case districts. While the magnitude of reclassification observed here for Tripoli and Benghazi (RR moving from 0.000 to approximately 0.03) is smaller than that reported in comparable Southeast Asian livestock studies where zero-case areas were reclassified to very high risk under the Poisson-Gamma model due to very low expected case counts (Hussin *et al*., 2026) the direction of the effect is consistent and theoretically expected, as Bayesian shrinkage toward the (non-zero) national base rate is more pronounced when the expected case count E_i is small relative to the prior's effective sample size. In the Libyan data structure used here, Tripoli and Benghazi have substantial exposed populations and correspondingly large expected counts ($E_i \approx 18.2\ and\ 15.8$ respectively), which limits the degree of upward correction the gamma prior can induce. Ghat, with a much smaller expected count ($E_i = 1.77$), exhibits a proportionally larger correction. This finding itself carries an important methodological implication. The magnitude of correction achievable through Poisson-Gamma smoothing is sensitive to the relative size of the expected case count, and districts with large cattle populations but persistent zero-reporting (such as Tripoli and Benghazi) warrant separate epidemiological scrutiny, as a true zero in a large population is a stronger signal than a true zero in a small one.

Both models robustly identified Zawiya and Jufra as the highest-risk districts in Libya, with Jafara and Zawara close behind as high-risk districts, a finding strongly consistent with the existing Libyan brucellosis literature. The elevated risk in the western coastal strip (Zawiya, Jafara, and Zawara) aligns with documented outbreak activity in northwest Libya following the post-2011 surveillance collapse (Al-Griw *et al*., 2017), where intensive small-ruminant and cattle husbandry, informal livestock trade, and degraded veterinary infrastructure combine to sustain transmission. The very high risk identified in Jufra district corroborates field seroprevalence findings from the Sokna locality, where extensive grazing practices and high animal concentration within oasis settlements were associated with a seroprevalence of 5.8 per cent, substantially higher than neighbouring Waddan and Hun (Alshekh *et al*., 2024). The medium-risk classification extended to Al-Koms, Jabal al-Gharbi, and Nalut under the Poisson-Gamma model further delineates a contiguous elevated-risk corridor spanning the entire western and northwestern regions of the country.

Brucella abortus disease mapping in Libya

The geographic distribution of *B. abortus* relative risk across all 22 districts was visualised using thematic maps based on the five-level RR classification described above, generated separately for the SMR method and the Poisson-Gamma model to allow direct visual comparison of the two estimation approaches.

Figure 5 presents the SMR-based thematic map for 2018 to 2024. Under this classification, Jufra ($RR = 4.737$) and Zawiya ($RR = 2.584$) are categorised as very high-risk districts, with Jafara ($RR = 1.837$) and Zawara ($RR = 1.595$) classified as high risk. Al-Koms, Jabal al-Gharbi, and Nalut (RRs between 1.015 and 1.102) are assigned to the medium-risk category. The remaining districts are mapped as low or very low risk. However, this SMR-based map assigns a sixth, distinct "no risk" category (shown in grey) to Tripoli, Benghazi, and Ghat, the three districts with zero reported cases a representation that does not distinguish between genuine absence of risk and a surveillance gap, despite Tripoli and Benghazi possessing substantial exposed cattle populations.

Figure 6 shows the corresponding thematic map based on the Poisson-Gamma model, which addresses this limitation by assigning a defensible, non-zero posterior risk estimate to every district, including those with zero reported cases. This adjustment resolves the visual ambiguity present in the SMR map: Tripoli ($RR = 0.027$), Benghazi ($RR = 0.032$), and Ghat ($RR = 0.282$) are now mapped within the "very low risk" category on a continuous risk scale, rather than appearing as a separate, qualitatively distinct "no risk" zone. Notably, Ghat's posterior estimate (0.282) is markedly higher than Tripoli's or Benghazi's, reflecting its smaller exposed population and correspondingly smaller expected case count, which allows the gamma prior proportionally greater influence a methodological nuance invisible on the SMR map. The high-risk corridor spanning Zawiya, Jufra, Jafara, and Zawara remains unchanged in classification between the two maps,

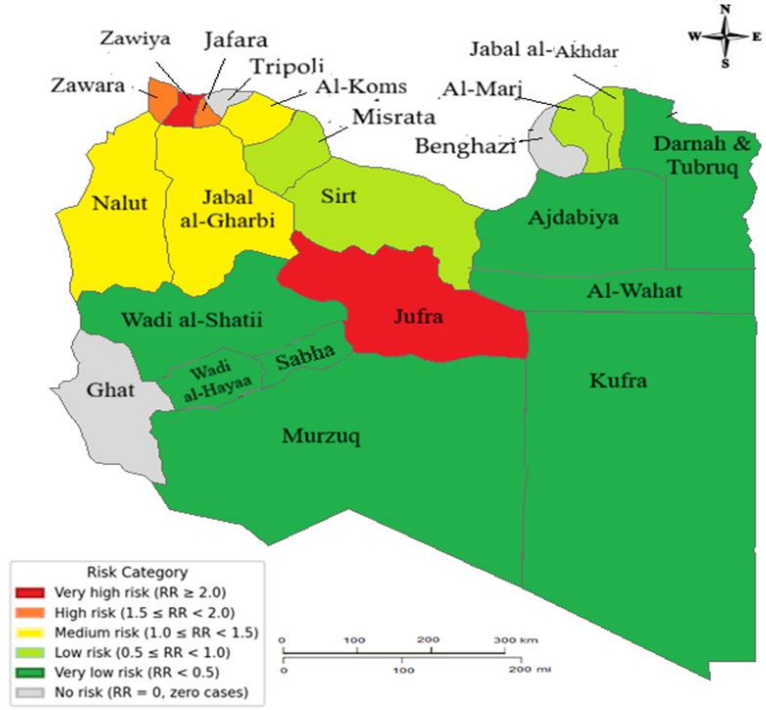


Figure 5. Standardized Mortality Ratio (SMR) method map for *B. abortus* cases during the years 2018 to 2024. Grey markers denote districts with zero reported cases, assigned a distinct "no risk" category under SMR.

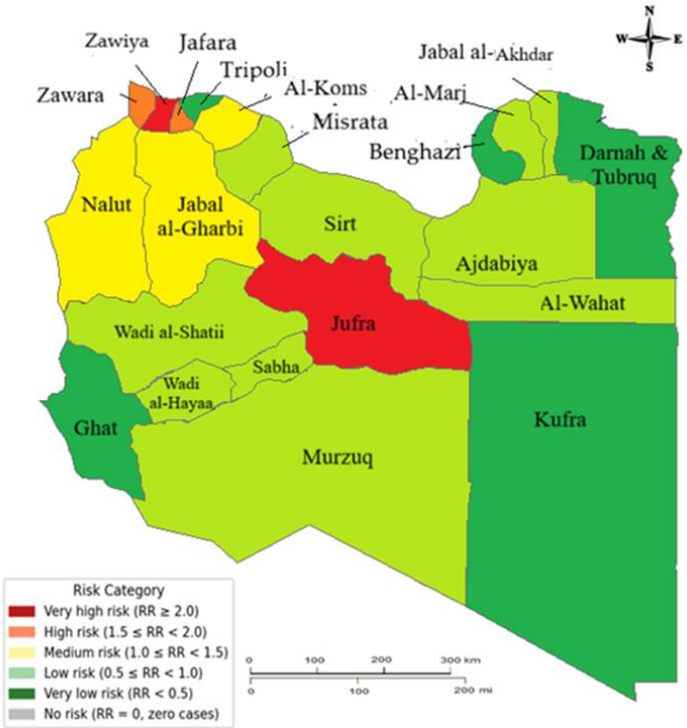


Figure 6. Poisson-Gamma model map for *B. abortus* cases during the years 2018 to 2024. All districts, including those with zero reported cases, are assigned a continuous, non-zero posterior risk estimate.

confirming the robustness of this finding to model choice. Although both models consistently identified Zawiya, Jufra, Jafara, and Zawara as the core high-risk corridor, the Poisson-Gamma map provides a more refined and policy-defensible spatial assessment, particularly for districts with sparse or zero-reported data. The elevated risk in the western coastal corridor may be associated with factors such as informal cross-

border livestock movement, high livestock density, and surveillance gaps (Al-Griw *et al*., 2017; Alshekh *et al*., 2024). In contrast, the low-to-very-low classifications across the southern Fezzan and eastern Cyrenaica periphery may reflect more extensive, lower-density grazing systems, geographic isolation, or comparatively under-resourced veterinary surveillance, a distinction the present data cannot fully resolve and that warrants targeted field investigation.

Contextualising these illustrative estimates against brucellosis research from neighbouring North African countries is instructive. In central-eastern Tunisia, Barkallah *et al*. (2017) reported a true individual-level cattle seroprevalence of 23.5% and herd-level prevalence of 55.6%, with *B. abortus* confirmed as a principal causative agent in cattle, figures far exceeding the below-0.2% national baseline cattle seroprevalence documented in Libya prior to 2011 (Al-Griw *et al*., 2017) and underscoring how substantially current Libyan case reporting likely understates true disease burden. In the Nile Delta region of Egypt, Hegazy *et al*. (2011) combined choropleth mapping with spatial scanning statistics across ten districts and 206 villages to identify localised clusters of elevated ruminant seroprevalence (approximately 12% in cattle and buffalo milk tanks), a methodological precedent supporting the use of smoothed, spatially explicit risk estimation, such as the Poisson-Gamma approach applied here, over raw-rate mapping in similarly data-sparse veterinary surveillance settings. In South-eastern Algeria, Ramdani *et al*. (2022) found small-ruminant brucellosis seropositivity concentrated in border districts and areas of high livestock density, a spatial clustering pattern broadly consistent with the elevated relative risk identified here in the western coastal and central oasis districts, which likewise combine high livestock density with cross-border trade exposure. Taken together, these regional findings reinforce the plausibility of the spatial patterns illustrated in this study and suggest that Libya's officially reported case numbers substantially understate true brucellosis burden relative to actively surveilled neighbouring countries.

Beyond its statistical performance, Bayesian disease mapping of this kind carries direct practical value for veterinary surveillance planning. By replacing unstable, zero-valued SMR estimates with smoothed, defensible relative-risk categories, the Poisson-Gamma approach allows veterinary authorities to rank districts for intervention even where reporting is incomplete, rather than mistakenly treating zero-case districts as risk-free. This supports a tiered allocation of limited diagnostic and vaccination resources, prioritising very high- and high-risk districts (Zawiya, Jufra, Jafara, and Zawara) for active surveillance, while flagging zero-reported-case districts (Tripoli, Benghazi, Ghat) for investigation of under-ascertainment rather than exclusion from planning. Because the method requires only routinely collected case counts and population denominators, together with modest computational resources (R or equivalent open-source software), it is readily implementable by national veterinary services and university-affiliated laboratories operating under the budget and infrastructure constraints typical of post-conflict settings, without requiring the individual-level covariate data needed for more complex spatial models. As such, the approach offers a practical, low-cost complement to WOAH-aligned reporting standards and a stepping stone toward more detailed spatial epidemiological surveillance once richer district-level data become available.

These spatial patterns are consistent with known risk factors for brucellosis transmission in the MENA region (Alramah, 2019; Samadi *et al*., 2024), including informal cross-border livestock movement along the Tunisian and Algerian borders proximate to the western coastal districts, unregulated consumption of unpasteurised dairy products in rural communities, and the lasting impact of disrupted vaccination and inspection regimes following the 2011 institutional collapse. The comparatively lower risk estimated for the southern Fezzan districts (Sabha, Murzuq, Wadi al-Hayaa, Wadi al-Shatii) and the remote southwestern district of Ghat may reflect both genuinely lower transmission intensity associated with more extensive, lower-density camel and small-ruminant husbandry, and potentially incomplete case ascertainment in these remote and sparsely populated regions, a distinction that the present data cannot resolve and that warrants targeted field investigation.

Sensitivity analysis of the Poisson-Gamma prior

To assess whether the informative-looking prior ($\alpha = 0.5$, $\beta = 0.0001$; Poisson-Gamma model section) unduly drives the reported relative-risk estimates, posterior RR_i values were recomputed for all 22 districts under three alternative gamma prior specifications spanning a wide range of informativeness: a weak prior ($\alpha = 1$, $\beta = 1$, prior mean 1, effective prior sample size 1), a Jeffreys-like prior ($\alpha = 0.5$, $\beta = 0.5$), and a near non-informative prior ($\alpha = 0.001$, $\beta = 0.001$). Table 3 reports the resulting RR_i for the three zero-case districts, the four core high-risk corridor districts, and one borderline district close to a risk-category threshold.

The core epidemiological finding of this study is robust to prior specification. All three zero-case districts (Tripoli, Benghazi, and Ghat) remain classified as very low risk, and all four core high-risk corridor districts (Zawiya, Jufra, Jafara, and Zawara) remain classified as very high or high risk, under every prior tested, including the near non-informative prior. Category reclassification occurred only for districts whose original RR_i estimate lay within approximately 0.01 of the Low/Very-low boundary (RR = 0.5), such as Al-Wahat, Sabha, Murzuq and Wadi al-Shatii, an expected consequence of proximity to a classification threshold rather than evidence of prior sensitivity in the substantive findings. This confirms that the priority districts identified for veterinary intervention are a robust feature of the data rather than an artefact of the specific hyperparameter values chosen.

Conclusion

This study compared the Standardized Mortality Ratio (SMR) method and the Poisson-Gamma model for estimating the relative risk of *B. abortus* in Libyan cattle populations from 2018 to 2024. The findings indicate that the Poisson-Gamma model provides a

Table 3. Sensitivity of posterior relative risk (RR_i) estimates to alternative gamma prior specifications in selected districts.

District	Original (α=0.5, β=0.0001)	Weak (α=1, β=1)	Jeffreys-Like (α=0.5, β=0.5)	Near Non-informative (α=0.001, β=0.001)	Risk Category Across Priors
Tripoli	0.027	0.052	0.027	0.000	Very low (all)
Benghazi	0.032	0.060	0.031	0.000	Very low (all)
Ghat	0.282	0.361	0.220	0.001	Very low (all)
Zawiya	2.614	2.491	2.536	2.583	Very high (all)
Jufra	4.853	4.052	4.361	4.740	Very high (all)
Jafara	1.861	1.798	1.817	1.837	High (all)
Zawara	1.632	1.555	1.575	1.595	High (all)
Al-Wahat	0.507	0.506	0.460	0.406	Low→Very low (2/3 alt.)

methodologically superior treatment of zero-case districts, correcting the SMR method's tendency to assign an absolute risk value of zero to areas such as Tripoli and Benghazi, where surveillance gaps, rather than genuine absence of disease, are the more plausible explanation for the lack of reported cases.

Both models consistently identified Zawiya and Jufra as very high-risk districts, with Jafara and Zawara as high-risk districts, comprising the priority districts for intensified veterinary surveillance and intervention identified across all 22 districts, a finding corroborated by independent Libyan seroprevalence research and visualised in the national thematic risk maps. These results support a risk-based, geographically targeted approach to brucellosis control in Libya, prioritising strengthened diagnostic capacity, livestock movement regulation, and vaccination coverage in the western coastal strip and central oasis districts identified as highest risk.

In practical terms, the Poisson-Gamma model is recommended for adoption by the Libyan veterinary authorities, for the foreseeable future, as the preferred tool for ongoing brucellosis surveillance, given its demonstrated robustness under conditions of incomplete and sparse data conditions that are likely to persist in the Libyan veterinary surveillance system. However, the present analysis should be understood as a methodological proof of concept rather than a definitive epidemiological assessment, given the illustrative nature of the district-level data employed. Future work should prioritise the acquisition of verified, disaggregated case data from the Libyan veterinary authorities or WOAH, the extension of the model to incorporate spatial correlation between neighbouring districts, and the integration of covariates such as livestock density, cross-border trade intensity, and veterinary service coverage to further refine risk estimation.

Conflict of interest

The author declares that there are no known competing financial interests or personal relationships that could have appeared to influence the work reported in this paper.

Data availability

The data supporting the findings of this study are available from the corresponding author upon reasonable request.

References

African Futures (ISS). (2024). Libya Development Futures: Geographic Profile. *Institute for Security Studies*. https://futures.issafrica.org/geographic/countries/liby/

Akoko, J.M., Mwatondo, A., Muturi, M., Wambua, L., Abkallo, H.M., Nyamota, R., & Bett, B. (2023). Mapping brucellosis risk in Kenya and its implications for control strategies in sub-Saharan Africa. *Scientific Reports*, 13(1), 20192.

Al-Afifi, A.H., Almashhadany, D.A., Al-Azazi, A.S., Khalaf, A.M., Odhah, M.N.A., & Al-Gabri, N.A. (2022). Prevalence of *Brucella spp.* in milk from aborted and non-aborted animals in Dhamar governorate, Yemen. *Italian Journal of Food Safety*, 11(4), 10370.

Al-Griw, H.H., Kraim, E.S., Farhat, M.E., Perrett, L.L., & Whatmore, A.M. (2017). Evidence of ongoing brucellosis in livestock animals in North West Libya. *Journal of Epidemiology and Global Health*, 7(4), 285–288. https://doi.org/10.1016/j.jegh.2017.09.001

Alramah, M.A. (2019). Mapping lung cancer disease in Libya using Standardized Morbidity Ratio, BYM model and mixture model, 2006 to 2011: a Bayesian epidemiological study. *Sains Malaysiana*, 48(1), 217–225. http://dx.doi.org/10.17576/jsm-2019-4801-25

Alshekh, K.A., Shahlol, A.M., Ben Mostafa, K.K., Othman, A.A., & Hiblu, M.A. (2024). Seroprevalence of brucellosis in sheep and goats from Al Jufrah district in Libya. *Pan African Medical Journal*, 48(23).

Barkallah, M., Gharbi, Y., Zormati, S., Karkouch, N., Mallek, Z., Gautier, M., Gdoura, R., & Fendri, I. (2017). A mixed methods study of ruminant brucellosis in central-eastern Tunisia. *Tropical Animal Health and Production*, 49(1), 39–45.

Central Intelligence Agency. (2026). Libya. *The World Factbook*. https://theworldfactbook.org/country/libya.html

Dadar, M., Tiwari, R., Sharun, K., & Dhama, K. (2021). Importance of brucellosis control programs of

livestock on the improvement of one health. *Veterinary Quarterly*, 41(1), 137–151.

Di Bari, C., Venkateswaran, N., Bruce, M., Fastl, C., Huntington, B., Patterson, G.T., & Devleesschauwer, B. (2022). Methodological choices in brucellosis burden of disease assessments: a systematic review. *PLoS Neglected Tropical Diseases*, 16(12), e0010468.

Diah, I.M., Aziz, N., & Kasim, M.M. (2017). A comparison of four disease mapping techniques as applied to TB diseases in Malaysia. *Journal of Telecommunication, Electronic and Computer Engineering (JTEC)*, 9(2-11), 133–137.

Flórez-Lozano, K., Navarro-Lechuga, E., Llinás-Solano, H., Tuesca-Molina, R., Sisa-Camargo, A., Mercado-Reyes, M., & Acosta-Reyes, J. (2020). Spatial distribution of the relative risk of Zika virus disease in Colombia during the 2015–2016 epidemic from a Bayesian approach. *International Journal of Gynecology & Obstetrics*, 148, 55–60.

Ghanbarnejad, A., Turki, H., Yaseri, M., Raeisi, A., & Rahimi-Foroushani, A. (2021). Spatial modelling of malaria in south of Iran in line with the implementation of the malaria elimination program: a Bayesian Poisson-Gamma random field model. *Journal of Arthropod-Borne Diseases*, 15(1), 108.

Ghssein, G., Ezzeddine, Z., Tokajian, S., Al Khoury, C., Kobeissy, H., Ibrahim, J.N., & Hassan, H.F. (2025). Brucellosis: bacteriology, pathogenesis, epidemiology and role of the metallophores in virulence: a review. *Frontiers in Cellular and Infection Microbiology*, 15, 1621230.

Grembi, J.A., & Rogawski McQuade, E.T. (2022). Introducing risk Communicator: an R package to obtain interpretable effect estimates for public health. *PLoS One*, 17(7), e0265368.

Hegazy, Y.M., Moawad, A., Osman, S., Ridler, A., & Guitian, J. (2011). Ruminant brucellosis in the Kafr El Sheikh Governorate of the Nile Delta, Egypt: Prevalence of a neglected zoonosis. *PLoS Neglected Tropical Diseases*, 5(1), e944.

Hussin, M.Z.M., Md Junus, N.W., Samat, N.A., & Muhid, A. (2026). Relative risk estimation for *Brucella abortus* in Malaysia: comparison of SMR and Poisson-Gamma disease mapping models. *Malaysian Journal of Fundamental and Applied Sciences*, 22(2), 309–320.

Jaya, I.G.N.M., & Folmer, H. (2020). Bayesian spatiotemporal mapping of relative dengue disease risk in Bandung, Indonesia. *Journal of Geographical Systems*, 22(1), 105–142.

Karim, M.R. (2024). Bayesian hierarchical spatial modeling of COVID-19 cases in Bangladesh. *Annals of Data Science*, 11(5), 1581–1607.

Khurana, S.K., Sehrawat, A., Tiwari, R., Prasad, M., Gulati, B., Shabbir, M.Z., & Chaicumpa, W. (2021). Bovine brucellosis—a comprehensive review. *Veterinary Quarterly*, 41(1), 61–88.

Laine, C.G., Johnson, V.E., Scott, H.M., & Arenas-Gamboa, A.M. (2023). Global estimate of human brucellosis incidence. *Emerging Infectious Diseases*, 29(9), 1789.

Lawson, A.B. (2006). Statistical methods in spatial epidemiology. Wiley. DOI: 10.1002/9780470035771

Lawson, A.B., Browne, W.J., & Rodeiro, C.L.V. (2003). Disease mapping with WinBUGS and MLwiN. John Wiley & Sons.

Libyan Heritage House. (2021). Topography of Libya. https://libyanheritagehouse.org/geography/topography-libya

Lokamar, P.N., Kutwah, M.A., Atieli, H., Gumo, S., & Ouma, C. (2020). Socio-economic impacts of brucellosis on livestock production and reproduction performance in Koibatek and Marigat regions, Baringo County, Kenya. *BMC Veterinary Research*, 16(1), 61.

Meza, J.L. (2003). Empirical Bayes estimation smoothing of relative risks in disease mapping. *Journal of Statistical Planning and Inference*, 112(1–2), 43–62.

Perez-Panades, J., Botella-Rocamora, P., & Martinez-Beneito, M.A. (2020). Beyond standardized mortality ratios; some uses of smoothed age-specific mortality rates on small areas studies. *International Journal of Health Geographics*, 19(1), 54.

Peterson, E., & Ver Hoef, J. (2014). STARS: an ArcGIS toolset used to calculate the spatial information needed to fit spatial statistical models to stream network data. *Journal of Statistical Software*, 56(1), 1–17.

Pinatt, J.M., Chicati, M.L., Ildefonso, J.S., & Filetti, C.R.G.D.A. (2020). Evaluation of pavement condition index by different methods: case study of Maringá, Brazil. *Transportation Research Interdisciplinary Perspectives*, 4, 100100.

Qureshi, K.A., Parvez, A., Fahmy, N.A., Abdel Hady, B.H., Kumar, S., Ganguly, A., & Aspatwar, A. (2023). Brucellosis: epidemiology, pathogenesis, diagnosis and treatment—a comprehensive review. *Annals of Medicine*, 55(2), 2295398.

Ramdani, N., Boussena, S., Bouaziz, O., & Moula, N. (2022). Brucellosis in small ruminant: Seroprevalence, risk factors, and distribution in the southeast of Algeria. *Tropical Animal Health and Production*. https://doi.org/10.1007/s11250-022-03236-1

Ribeiro, M., Azevedo, L., & Pereira, M.J. (2024). EpiGeostats: an R package to facilitate visualization of geostatistical disease risk maps. *Mathematical Geosciences*, 56(1), 103–119.

Samadi, A., Amiri, M., & Hailat, N. (2024). The reasons behind long-term endemicity of brucellosis in low and middle-income countries: challenges and future perspectives. *Current Microbiology*, 81(3), 82.

Samat, N.A., & Percy, D.F. (2012). Dengue disease mapping in Malaysia based on stochastic SIR models in human populations. In 2012 International Conference on Statistics in Science, Business and Engineering (ICSSBE), pp. 1–5. IEEE.

Sharma, V., Singh, B.B., & Brookes, V.J. (2025). Risk assessment of Brucella exposure through raw milk consumption in India: One Health implications and control strategies. *Veterinary Sciences*, 12(5), 465.

Copyright Author (s) 2026.
Distributed under Creative Commons CC-BY 4.0